

# Assessment of Vessel Tortuosity in Retinal Images of Preterm Infants

Faraz Oloumi<sup>1</sup>, Rangaraj M. Rangayyan<sup>1\*</sup>, and Anna L. Ells<sup>1,2</sup>

**Abstract**—Diagnosis of plus disease is crucial for timely treatment and management of retinopathy of prematurity. An indicator of the presence of plus disease is an increase in the tortuosity of blood vessels in the retina. In this work, we propose a new angle-variation-based measure for quantification of tortuosity in retinal fundus images of preterm infants. The methods include the use of Gabor filters to detect vessels as well as to obtain their orientation at each pixel. Morphological image processing methods are used to obtain a skeleton image of the vessels for measurement of tortuosity. Out of 11 vessel segments, marked by an expert ophthalmologist as showing high levels of tortuosity due to plus disease, all were correctly identified using the proposed methods.

## I. INTRODUCTION

### A. Retinopathy of Prematurity

Retinopathy of prematurity (ROP) is a retinal disorder that affects the development of vasculature in preterm infants. ROP is the leading cause of preventable childhood blindness [1]. Infants with low birth weight and gestational age are required to be screened for ROP [2]. In a screening program of nearly 7,000 preterm infants in the Early Treatment for ROP study, about 68% of the infants were observed to develop ROP [3]. In recent years, it has been established that treatment and management of ROP should be based on the presence of plus disease [4], [5], which is clinically diagnosed by the presence of a certain level of venular dilation and increased arteriolar tortuosity [1]. However, determination of the sufficient amount of increase in thickness and tortuosity is done by qualitative comparison with a gold-standard image, which is said to be atypical since it shows more vascular dilation and less tortuosity as compared to most cases with plus disease [5].

The diagnosis of plus disease based on the current clinical methods is subjective. According to a study setup to assess the interexpert agreement of plus disease diagnosis based on 3-level classification (normal, abnormal, and plus), the experts agreed on the diagnosis of only 12% of the images (4 out of 34) [6]. Such studies show the need for methods to quantify the changes in blood vessels, such as tortuosity, in the presence of plus disease.

Unlike thickness, tortuosity does not have a formal definition; there have been several different methods proposed for representation and quantification of tortuosity in the literature. It is important to note that, to measure tortuosity, a skeletal representation of the vasculature is required. Such

representation of the vasculature could be obtained either manually or by using automated image processing methods. All of the methods presented in the literature use manual segmentation or selection of vessels for the measurement of tortuosity in the presence of plus disease.

The most simple and widely used measure of tortuosity is defined as the ratio between the total length of a vessel segment and its chord (the line connecting the endpoints of the vessel segment) [7]–[9].

Grisan et al. [10] used curvature to divide a vessel segment into straight and curved parts. They defined the tortuosity of a given vessel segment as the normalized sum of length-to-chord measures of the curved and straight parts as previously obtained using curvature.

Chandrinios et al. [11] proposed a measure of tortuosity based on the direction of vectors constructed using the coordinates of skeleton pixels. Given a pixel under consideration,  $P$ , the two vectors connecting  $P$  with its previous and next pixels were constructed and divided by their norms. The tortuosity index of pixel  $P$  was defined as the inverse cosine of the dot product of the two vectors. The tortuosity measure was summed over all available pixels in a vessel segment and then divided by the length of the segment.

Given a skeleton of the vasculature, Poletti et al. [12] proposed an angle-based tortuosity measure by first defining the angle of a given pixel based on the coordinates of the current and previous pixels. The local change in angle was then defined as the difference in the inverse tangent of the angle of the current and previous pixels. The tortuosity measure was computed as the sum of the squared angle changes, divided by the total length of the vessel segment.

The drawback of the length-to-chord measure [7] is that an arched segment (not tortuous) and a sinusoidal segment (tortuous) with the same total and chord lengths will lead to equal tortuosity measures. The angle-based measures proposed by Chandrinios et al. [11] and Poletti et al. [12] are computed using only the skeleton of the vasculature, which, due to errors in detection, segmentation, and quantization, could lead to inaccurate computation of the orientation of a given pixel based on the coordinates of the skeleton pixels. Furthermore, the method of Poletti et al. [12] defines the orientation of a given pixel by considering only the previous pixel's location and is independent of the location of the next pixel. In this work, we propose a new angle-variation-based tortuosity (AVT) measure based on the angle information provided by the Gabor filters used for the detection of vessels, which provide a more accurate representation of the orientation of the vessels.

<sup>1</sup>Department of Electrical and Computer Engineering, Schulich School of Engineering, University of Calgary, Calgary, AB, Canada, T2N 1N4. \*ranga@ucalgary.ca.

<sup>2</sup>Division of Ophthalmology, Department of Surgery, Alberta Children's Hospital, Calgary, AB, Canada, T3B 6A8.

## II. MATERIALS AND METHODS

### A. Retinal Fundus Images

The proposed methods were tested with several retinal fundus images from the Telemedicine for ROP In Calgary (TROPIC) database [13]. The images of the TROPIC database were captured using the RetCam 130 camera [wide-field (130°)] and have a size of  $640 \times 480$  pixels. The spatial resolution of the RetCam 130 images is estimated to be  $30 \mu\text{m}/\text{pixel}$  [14]. Five images showing no signs of plus disease and two images diagnosed with plus disease were used in the present pilot study. In total, 11 vessel segments were identified by an expert ophthalmologist and retinal specialist (A.L. Ells) as showing sufficient tortuosity to indicate the presence of plus disease. The 11 vessel segments are used in the present work to assess the potential of the proposed method. In addition, the methods were tested with three images showing tortuosity that was not adequate for the diagnosis of plus disease but could possibly be considered as indicators of preplus disease.

### B. Detection of Blood Vessels

In the present work, real Gabor filters are used for the detection of blood vessels. Gabor filters are sinusoidally modulated Gaussian functions that are sensitive to oriented features. A single-scale Gabor filter has been shown to provide high accuracy in the detection of retinal blood vessels [15]. The frequency response of the main Gabor filter oriented at  $\theta = -\pi/2$  is given as

$$G(u, v) = \frac{1}{2} \left( \exp \left[ -2\pi^2 \{ \sigma_x^2 (u + f_o)^2 + \sigma_y^2 v^2 \} \right] + \exp \left[ -2\pi^2 \{ \sigma_x^2 (u - f_o)^2 + \sigma_y^2 v^2 \} \right] \right), \quad (1)$$

where  $f_o$  is the frequency of the modulating sinusoid and  $\sigma_x$  and  $\sigma_y$  are the standard deviation values in the  $x$  and  $y$  directions, respectively. For simplicity of design and use, two parameters for thickness ( $\tau$ ) and elongation ( $l$ ) are defined such that  $\sigma_x = \tau/(2\sqrt{2}\ln 2)$ ,  $\sigma_y = l\sigma_x$ , and  $f_o = 1/\tau$ . A bank of  $K$  equally spaced filters over the range  $[-\pi/2, \pi/2]$  is obtained by rotating the filter response given in Equation 1.

The magnitude output of the Gabor filter is obtained by taking the maximum filter response over all angles for each pixel. The orientation of the filter at a given pixel with the maximum response is recorded as the orientation of the vessel at the pixel.

### C. Measurement of Angle-Variation-Based Tortuosity

The magnitude response of the Gabor filters is binarized and short, unconnected segments (mostly related to choroidal vessels) that are left behind after the binarization step are removed using the morphological operation of area open. The binary image is then skeletonized and spurs of up to 5 pixels are removed. Branching points on the skeleton are identified and removed to break apart vessel segments. Short, broken segments with length less than  $450 \mu\text{m}$  (15 pixels)

are removed. Each segment of the skeleton is then labeled using a number and the AVT is computed for each segment.

We propose a new angle-variation index (AVI) based on the Gabor angle at a given pixel as

$$\text{AVI}(p) = \frac{1}{2} \left\{ \left| \sin [\phi(p) - \phi(p-1)] \right| + \left| \sin [\phi(p) - \phi(p+1)] \right| \right\}, \quad (2)$$

where  $p$ ,  $p-1$ , and  $p+1$  are the current, previous, and next pixels, respectively, along a vessel segment, and  $\phi$  denotes the Gabor angle. This formulation ensures that the AVI has a theoretical maximum value of 1 and a minimum of 0 at each pixel. The AVT for a given vessel segment is then defined as  $\text{AVT} = \frac{1}{N} \sum_{n=1}^N \text{AVI}(n)$ , where  $N$  is the total number of pixels in the segment. The AVT is normalized, so that it provides a maximum value of 1 and a minimum of 0 for each vessel segment.

In clinical practice, retinal images are classified into three categories of normal, abnormal, and plus. In order to facilitate a similar representation using the AVT measure, two thresholds are used to classify each vessel segment and the results are displayed using color coding. High levels of tortuosity associated with plus disease are shown in red, abnormal levels of tortuosity that are not sufficient for the diagnosis of plus disease in yellow, and normal or low levels in green. In this work, threshold values used to divide the AVT measure into three categories were set to 0.06 and 0.03.

In the present work, values of  $\tau = 7$  pixels,  $l = 1$ , and  $K = 180$  were used to obtain the Gabor magnitude and angle responses for all fundus images. The threshold used to binarize each vessel image was selected interactively using a graphical user interface designed for the purpose of implementation and application of the proposed methods in a clinical setting. The binarization step is the only manually performed step in the entire procedure used to derive AVT.

## III. RESULTS

### A. Evaluation of the AVT Measure

In order to evaluate the proposed AVT measure, a test image containing nine line segments representing various forms of vessels was created. Eight segments are sinusoids with varying frequencies (two of which are damped) and one segment is a straight line. In order to divide the segments into three categories, as explained in the previous section, thresholds of  $\text{AVT} = 0.05$  and  $0.025$  were used.

Fig. 1 illustrates the test image after derivation of the AVT measure and color coding the segments based on their level of tortuosity. Values of  $\tau = 5$  pixels,  $l = 1$ , and  $K = 180$  were used to apply Gabor filters to the test image. It is evident that the segments are correctly identified in terms of their increasing tortuosity, with the three segments with the highest frequencies colored red, and the two with the lowest frequencies as well as the straight line colored green.

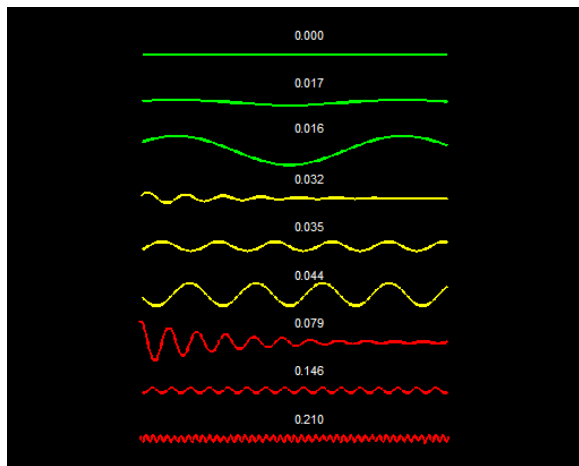


Fig. 1. A test image of size  $640 \times 480$  pixels representing skeletons of vessels using sinusoids and a straight line. Assuming a pixel size of  $30 \mu m$ , the frequency of the sinusoids from top to bottom (excluding the straight line) are: 1.32, 1.32, 7.94, 5.29, 4.5, 10.75, 15.87, and 41.67 cycles/mm. The AVT value obtained for each segment is shown on the image. The skeletons have been dilated using a disk of radius one pixel for better illustration.

### B. Application of AVT to Retinal Images

Fig. 2 (a) illustrates a normal case showing no signs of plus disease. Part (b) of the same figure shows the color-coded skeleton image obtained using the proposed methods. All segments are either colored green or yellow, indicating the absence of highly tortuous vessel segments.

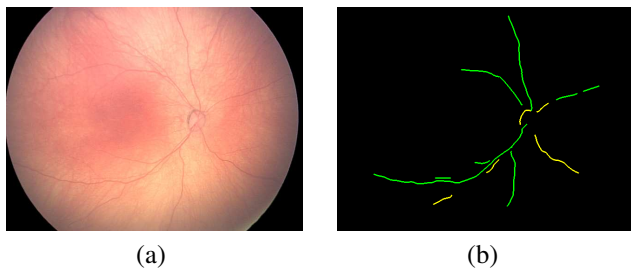


Fig. 2. (a) Image 2701 of the TROPIC database which does not show any sign of plus disease. (b) The color-coded skeleton image of (a) obtained using the proposed methods. The skeleton image has been dilated using a disk of radius one pixel for better illustration.

Fig. 3 shows an image with signs of plus disease including tortuous vessels. All vessels marked by the specialist as being sufficiently tortuous to indicate the presence of plus disease have been correctly marked in red. However, the method also indicates the presence of other vessel segments that have provided similar AVT values compared to the segments marked by the specialist.

All of the 11 tortuous vessel segments that were marked by the specialist in two images associated with plus disease were correctly identified by the proposed AVT method as showing high levels of tortuosity. One of the images indicating plus disease has poor contrast; therefore, the vessel detection and binarization steps were not capable of detecting all available vessel segments. As a result, parts of the vessels that were

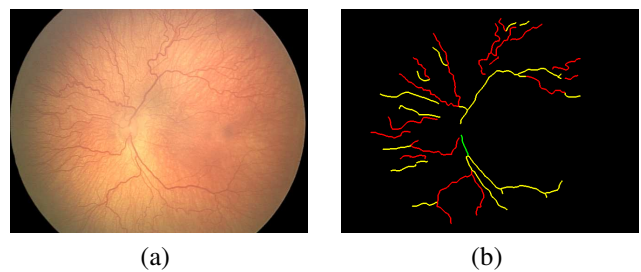


Fig. 3. (a) Image 2203 of the TROPIC database; the corresponding patient was diagnosed with plus disease based on the presence of vascular dilation and increased tortuosity. (b) The color-coded skeleton image of (a) obtained using the proposed methods. The skeleton image has been dilated using a disk of radius one pixel for better illustration.

marked by the specialist were missed in the final results. In the set of five normal images analyzed all segments were marked green or yellow. In the three images categorized as preplus, a total of 30 vessel segments were marked yellow and 14 were marked red.

## IV. DISCUSSION AND CONCLUSION

The proposed methods correctly identified all 11 tortuous vessel segments in two fundus images that were marked by a retinal specialist as possessing high levels of tortuosity. In addition, the methods classified all vessels in the five normal images analyzed as not being sufficiently tortuous to indicate the presence of plus disease.

The AVT measure is superior to the length-to-chord measure because it is capable of detecting local changes in curvature, whereas the latter is only sensitive to global changes on a curve. Compared to other angle-based tortuosity measures, the AVT measure is more accurate since it employs Gabor angle information, which is obtained at the vessel detection level and is more accurate than estimating the angle of a vessel pixel using the skeleton that is prone to approximation and quantization errors. The definition of AVT also ensures that the final measure is normalized to allow for comparison of vessel segments of various lengths.

Even though the results are encouraging, a few issues need to be addressed. If a vessel is composed of a relatively long straight segment and a short tortuous segment, the AVT measure may average out the large AVI values indicating high tortuosity and lead to an overall result that does not accurately represent the tortuous parts of the vessel. By using a sliding window to analyze the variation in AVI within appropriate lengths of vessels, it should be possible to ignore the straight parts of a vessel and correctly identify the tortuous parts.

In clinical practice, the amount of vessel tortuosity that is not considered to be adequate for plus diagnosis is indicated by the term preplus. As mentioned in Section I-A, such distinction is subjective. The thresholds used to separate the AVT measure into appropriate categories is a crucial step. In order to determine suitable thresholds for the value of AVT to indicate the presence of plus or preplus disease, a training

set of images of plus and preplus cases where the tortuous vessels are marked is required.

All published studies dealing with measurement of vessel tortuosity and dilation in images of preterm infants have intentionally selected images with the highest quality and contrast in order to minimize the errors introduced as a result of low quality. However, in reality and in clinical practice, such discrimination is not feasible and the available images may possess low contrast and suffer from movement artifacts. The images used in this preliminary study, and a larger set of 110 images being prepared for further studies, have been selected from the TROPIC database without such discrimination and are used in this work to analyze the robustness of the proposed methods.

The methods developed in the present work are fully automated, except for the binarization step and the initial removal of small segments using the area open procedure. Eight automated thresholding methods were studied and employed to obtain binary images of retinal vessels. However, due to the variable nature of the retinal images of preterm infants, such as low contrast, varying pigmentation, and blurring effects, no single automated thresholding method provided consistent results for binarization of all images. Combination of the results of multiple thresholding methods may lead to better binarization results; this is a work in progress.

There have been various semiautomated computer-aided programs developed that have tried to perform diagnosis of plus disease by quantification of the changes in tortuosity of retinal blood vessels [8], [9]. The methods used involve manual marking of vessel segments, or manual selection of parts of automatically detected vessels to include only the desired vessels for further analysis. Such manual input can bias the final result. The methods presented in the present work are capable of distinguishing all tortuous vessels present in a given image without any manual selection.

Most studies dealing with the diagnosis of plus disease only analyze the major branches of retinal vessels close to the posterior pole, i.e., near the ONH. However, as shown by Keck et al. [16], the indication of plus disease is stronger when tortuosity is observed farther away from the optic nerve head (ONH). The present work does not limit the area of analysis or the types of vessels that are analyzed.

The clinical diagnosis of plus disease requires tortuosity to be present in at least two quadrants of the retinal image. However, all studies in the literature dealing with quantification of tortuosity provide a single average value of tortuosity for the entire image. Analyzing all of the available vessels and providing an average measure may result in a washout effect. It is important to integrate the clinical approach for diagnosis with the available methodology for quantitative image analysis to derive suitable criteria for computer-aided diagnosis (CAD) of plus disease based on tortuosity. For instance, given the center of the ONH, the fundus image could be divided into four quadrants and the average AVT of all vessels labeled red (highly tortuous) in each quadrant could be considered for diagnosis, only if the averages are

above the threshold in at least two quadrants.

We have proposed a novel method for quantification of tortuosity of retinal vessels based on variations in the angle of blood vessels obtained using Gabor filters, which can be used in a CAD system for diagnosis of plus disease.

#### ACKNOWLEDGMENT

This work was supported by the Natural Sciences and Engineering Research Council of Canada. We thank April Ingram for help with the TROPIC database.

#### REFERENCES

- [1] International Committee for the Classification of Retinopathy of Prematurity, "The international classification of retinopathy of prematurity revisited," *Arch Ophthalmol*, vol. 123, pp. 991–999, 2005.
- [2] A. L. Ells, M. Hicks, M. Fielden, and A. D. Ingram, "Severe retinopathy of prematurity: longitudinal observation of disease and screening implications," *Eye*, vol. 19, no. 12, pp. 138–144, 2005.
- [3] Early Treatment for Retinopathy of Prematurity Cooperative Group, "The incidence and course of retinopathy of prematurity: Findings from the early treatment for retinopathy of prematurity study," *Pediatrics*, vol. 116, no. 1, pp. 15–23, 2005.
- [4] Early Treatment for Retinopathy of Prematurity Cooperative Group, "Revised indications for the treatment of retinopathy of prematurity: Results of the early treatment for retinopathy of prematurity randomized trial," *Arch Ophthalmol*, vol. 121, pp. 1684–1696, 2003.
- [5] B. V. Davitt and D. K. Wallace, "Plus disease," *Surv Ophthalmol*, vol. 54, no. 6, pp. 663–670, Nov-Dec 2009.
- [6] M. F. Chiang, L. Jiang, R. Gelman, Y. E. Du, and J. T. Flynn, "Interexpert agreement of plus disease diagnosis in retinopathy of prematurity," *Arch Ophthalmol*, vol. 125, no. 7, pp. 875–880, 2007.
- [7] W. Lotmar, A. Freiburghaus, and D. Bracher, "Measurement of vessel tortuosity on fundus photographs," *Albrecht von Graefes Archiv für klinische und experimentelle Ophthalmologie*, vol. 211, no. 1, pp. 49–57, 1979.
- [8] S. Koreen, R. Gelman, M. E. Martinez-Perez, L. Jiang, A. M. Berrocal, D. J. Hess, J. T. Flynn, and M. F. Chiang, "Evaluation of a computer-based system for plus disease diagnosis in retinopathy of prematurity," *Ophthalmology*, vol. 114, no. 12, pp. 59–67, 2007.
- [9] C. M. Wilson, K. D. Cocker, M. J. Moseley, C. Paterson, S. T. Clay, W. E. Schulenburg, M. D. Mills, A. L. Ells, K. H. Parker, G. E. Quinn, A. R. Fielder, and J. Ng, "Computerized analysis of retinal vessel width and tortuosity in premature infants," *Invest Ophthalmol Vis Sci*, vol. 49, no. 1, pp. 3577–3585, 2008.
- [10] E. Grisan, M. Foracchia, and A. Ruggeri, "A novel method for the automatic grading of retinal vessel tortuosity," *IEEE Trans Med Imaging*, vol. 27, no. 3, pp. 310–319, March 2008.
- [11] K. V. Chandrinos, M. Pilu, R. B. Fisher, and P. E. Trahanias, "Image processing techniques for the quantification of atherosclerotic changes," in *Proc. MEDICON98*, Cyprus, Greece, June 1998.
- [12] E. Poletti, E. Grisan, and A. Ruggeri, "Image-level tortuosity estimation in wide-field retinal images from infants with retinopathy of prematurity," in *Proc. IEEE Eng Med Biol Soc Conference*, San Diego, CA, 2012, pp. 4958–4961.
- [13] P. L. Hildebrand, A. L. Ells, and A. D. Ingram, "The impact of telemedicine integration on resource use in the evaluation ROP ... analysis of the telemedicine for ROP in Calgary (TROPIC) database," *Invest Ophthalmol Vis Sci*, vol. 50, pp. E-Abstract 3151, 2009.
- [14] D. J. De Silva, K. D. Cocker, G. Lau, S. T. Clay, A. R. Fielder, and M. J. Moseley, "Optic disk size and optic disk-to-fovea distance in preterm and full-term infants," *Invest Ophthalmol Vis Sci*, vol. 47, no. 11, pp. 4683–4686, 2006.
- [15] R. M. Rangayyan, F. J. Ayres, Faraz Oloumi, Foad Oloumi, and P. Eshghzadeh-Zanjani, "Detection of blood vessels in the retina with multiscale Gabor filters," *J Electron Imaging*, vol. 17, pp. 023018:1–7, April-June 2008.
- [16] K. M. Keck, J. Kalpathy-Cramer, E. Ataer-Cansizoglu, S. You, D. Erdogmus, and M. F. Chiang, "Plus disease diagnosis in retinopathy of prematurity: Vascular tortuosity as a function of distance from optic disk," *Retina*, vol. 33, no. 8, pp. 1700–1707, 2013.